Bimetallic Silver-Gold Clusters by Matrix-Assisted Laser Desorption/Ionization

Sándor Kéki, Lajos Nagy, György Deák, and Miklós Zsuga
Department of Applied Chemistry, University of Debrecen, Debrecen, Hungary

Pure gold clusters (Au_n^+) were produced up to the cluster size of n = 100 by matrix-assisted laser desorption/ionization (MALDI). The mass spectrum of the resulting clusters showed alteration in the ion intensity at odd-even clusters size. On the other hand, intensity drops at cluster size predicted by the jellium model theory was also observed. Positively and negatively charged bimetallic silver-gold clusters were produced under MALDI conditions from the mixture of $HAuCl_4$/silver trifluoroacetate and the 2-(4-hydroxyphenylazo)benzoic acid (HABA) matrix. A linear correlation was found between the intensity ratio of $Au_nAg_m^+$ to $Au_{n+1}Ag_{m-1}^+$ cluster ions and the molar ratio of the gold to silver salt. It was observed that the composition and the distribution of the clusters can be varied with the molar ratio of the silver and gold salts. It was also found that the resulting cluster sizes obey the lognormal distribution. (J Am Soc Mass Spectrom 2004, 15, 1455–1461) © 2004 American Society for Mass Spectrometry

Clusters containing atoms up to a few thousands represent an intermediate between single atom and bulk materials. Besides fundamental interest, extensive study of such species over the past decades has been motivated by their potential technological application in areas such as optics [1, 2], catalysis [3, 4], and photography [5]. Metal clusters containing two different kinds of atoms, that is, binary clusters or nano-alloys have received growing interest since they are regarded as small scale precursors of bulk alloys. The variation of the atom types building up the cluster and/or the composition, as well as the size of the cluster offers various possibilities to engineer their properties for specific technological and scientific demands. However, to achieve these specific goals much information on the physical and chemical properties of the clusters as the function of their composition and size should be gained. Mass spectrometric methods provide a unique experimental tool for the investigation of the electronic and geometric properties of small-size metal clusters [6].

In the past decades several methods were explored to induce gas-phase generation of metal clusters, and most of these techniques were based on the evaporation of metals by heating [7, 8], or using laser ablation [9–11] and ion-bombardment [12–15]. The production and investigation of binary silver-gold [2, 16, 17] and those of the pure silver [12–14, 18] and gold clusters [12, 13] has been reported by several research groups. However, in contrast to the information available on the pure silver and gold clusters, only very limited experimental [16, 17] and theoretical studies [19] on the properties of small size silver-gold clusters have been reported. Recently, the generation of silver-cluster ions in matrix-assisted laser desorption/ionization (MALDI) [20, 21] was reported using silver salts and various matrixes [22–24]. In a previous paper [24] we have shown that both positively and negatively charged silver clusters up to the size of 200 can be effectively produced from silver ions under MALDI conditions. It was noted that considerable reduction of Ag^+ takes place in the plume and the matrices enhance the formation of silver clusters. As a continuation of our work, we utilized this method for the generation of pure gold clusters and for the production of mixed binary gold-silver clusters. To our best knowledge we are the first to apply the MALDI method to produce pure gold and bimetallic Au-Ag cluster ions. The present report shows that the resulting distribution of the binary gold-silver clusters can be effectively changed with the initial molar ratio of the silver and gold salt.

Experimental

Materials

2-(4-Hydroxyphenylazo)benzoic acid (HABA) and silver trifluoroacetate (AgTFA) were purchased form Aldrich (Taufkirchen, Germany) and used as received. $HAuCl_4$ was received from Reanal (Budapest, Hungary) and used without further purification. Tetrahydrofuran (THF) from Aldrich was purified as described [25].

Instruments

MALDI-TOF MS. The MALDI MS measurements were performed with a Bruker BIFLEX III mass spec-

Published online September 11, 2004

Address reprint requests to Professor M. Zsuga, Applied Chemistry, University of Debrecen, Egyetem ter 1., H-4010 Debrecen, Hungary. E-mail: zsugam@tigris.klte.hu

1044-0305/04/$30.00
doi:10.1016/j.jasms.2004.07.001

Received March 25, 2004
Revised June 11, 2004
Accepted July 2, 2004

trometer (Bremen, Germany) equipped with a TOF analyzer. In all cases 19 kV total acceleration voltage was used with a 3 kV pulse (extraction) voltage and with a delay time of 300 ns. The ions were detected in the reflectron mode. An LSI type nitrogen laser (337 nm, 3 ns pulse width) operating at 2 Hz was used to produce laser desorption and 500 shots were summed. The matrix was dissolved in THF at a concentration range of 20 mg/mL. AgTFA and $HAuCl_4$ were dissolved in THF at concentrations of 39 and 20 mg/mL. It should be noted that the solutions of the silver and gold salts were separately mixed with the matrix solution, and this way no precipitation of AgCl was observed during sample preparation. The ions were detected with a multi-channel plate (MCP) detector at the voltage of 1.65 kV. The spectra were externally calibrated with poly(ethylene glycol) (PEG) (M_n = 1450 g/mol, M_w/M_n = 1.02). The solutions of the matrix, AgTFA and $HAuCl_4$ were mixed in a 5:1 vol/vol ratio (matrix: salts). A volume of 0.5 μl of these solutions was deposited onto the sample plate (stainless steel), and allowed to air-dry.

Post-source decay (PSD) MALDI-TOF MS/MS. All of the PSD spectra were recorded by selection of the precursor ion to be studied, using the pulser allowing an approximately 20 Da window for selection. In these experiments 19 kV total acceleration voltage and 4.55 kV pulse voltage with a delay time of 100 ns were employed. In each segment of the spectrum accumulation, the reflectron voltage was decreased. The segments were pasted and calibrated using an XMASS 5.0 software from Bruker. The PSD was calibrated using the fragmentation pattern of adrenocorticotropic hormone (ACTH) over the mass range of 60–2450 Da.

Fitting method and software. For fitting the parameters of the lognormal distribution to the experimental data a home-made computer program called Fitter5v utilizing the Gauss-Newton-Marquardt procedure was used [26].

Supplementary materials. The full MALDI-TOF MS spectrum of a mixture of HABA, AgTFA and $HAuCl_4$ recorded in the positive (**a**) and in the negative (**b**) reflectron mode and the intensity ratios of Au_nAg_{k-n} to $Au_{n-1}Ag_{k-n+1}$ versus n_{Au}/n_{Ag} for the negatively charged cluster ions as well as the normalized ion intensities of the negatively charged cluster ions as a function of the number of Au atoms and the cluster size are available from the Authors upon request.

Results and Discussion

Generation of Pure Gold Cluster Ions Under MALDI Conditions

In a previous work [24] we have shown that high silver cluster ions up the mass of 22,000 Da can be produced from the mixture of HABA/silver trifluoroacetate. We

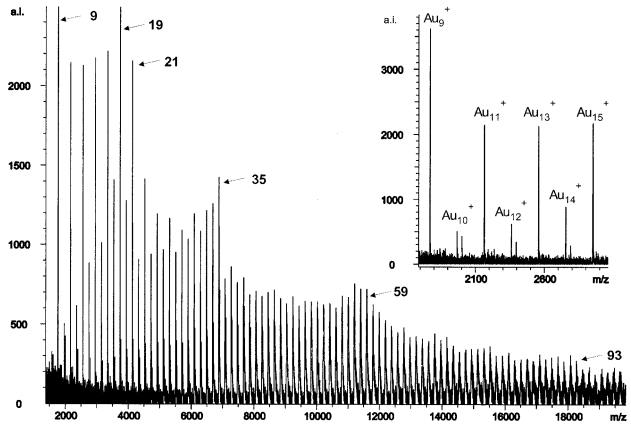

Figure 1. The positive reflectron MALDI-TOF MS spectrum obtained with the mixture of HABA and $HAuCl_4$. Experimental conditions: 5:1 (vol/vol) mixture of HABA (20 mg/mL) and $HAuCl_4$ (20 mg/mL) solutions.

applied this method to generate gold clusters using HABA as the matrix and $HAuCl_4$ salt as the source of clusters. The reflectron MALDI-TOF MS spectrum obtained with the mixture of HABA/$HAuCl_4$ is shown in Figure 1. It should be mentioned, however, that the spectrum in Figure 1 was accumulated in a way that ions below *m/z* 700 (matrix, adduct ions, and small gold cluster ions) were deflected to avoid saturation of the detector due to the high intensity of these ions. As seen in Figure 1, a series of peaks with a repeat mass of 197 Da appeared, which is characteristic of the average mass of gold. On the other hand, only single isotopic peaks were found for the clusters with masses up to 3000 Da (isotopic resolutions were achieved in this mass range), which is indicative of the gold. These findings prove the presence of Au_n^+ cluster ions. Figure 1 also shows that the spectrum has two particular properties: (1) the ion intensities alternate at odd-even cluster sizes, that is, the ion intensity of the odd clusters is higher than that of the adjacent even number clusters; (2) the ion intensity decreases sharply at cluster numbers called "magic" numbers. The magic numbers observed in this work are n = 9, 19, 21, 35, 59, and 93. These observations can be interpreted in terms of the jellium model [6, 12, 13]. According to this theory, the stability of the cluster is particularly dependent on the energy levels of the free electrons located in the cluster. Therefore, clusters with even-number valance electrons are more stable, due to spin-spin coupling, than those having odd-number of electrons. On the other hand, clusters with a closed electronic shell possess higher stability than those of the neighboring. The shell-closures occur at number of free electrons n_s = 2, 8, (18), 20, 34, 40, 58, 92, 138. For the single positively charged clusters these numbers occur at the magic numbers $n_m = n_s+1$, in good accordance with the experimental ones. Interestingly, magic number 41 was not observed in the case of gold, but magic number 19 seems to be prominent. Our observations under MALDI conditions

are in accordance with those obtained with gold clusters by another method [12, 13]. It should be noted, that the formation of single negatively charged Au_n^- cluster ion was also observed, but the signal intensity was very weak as compared to that of Au_n^+. Since the Au_n^+ and Au_n^- cluster ions were generated with MALDI in the presence of HABA matrix, formation of hydride type ions, e.g., Au_nH^+ is also possible as suggested by one of our reviewers. In the low mass region (1000–3000 Da) the presence of these hydride ions can be excluded (mass accuracy is within 0.3 Da in this mass range), however, at high masses, due to the low signal to noise ratio and low mass accuracy, their presence cannot be excluded. We have reported in a previous paper on the MALDI-generated silver clusters [24] that considerable reduction of the metal ions takes place in the plume, and this is also the case in the present situation. Since the formation of negatively charged cluster ions requires higher flux of electrons that is supplied by the matrix, lower signal intensity in the negative mode can be expected in good agreement with the experimental results. On the other hand, the matrix acts as a moderator to enhance the growth of the clusters.

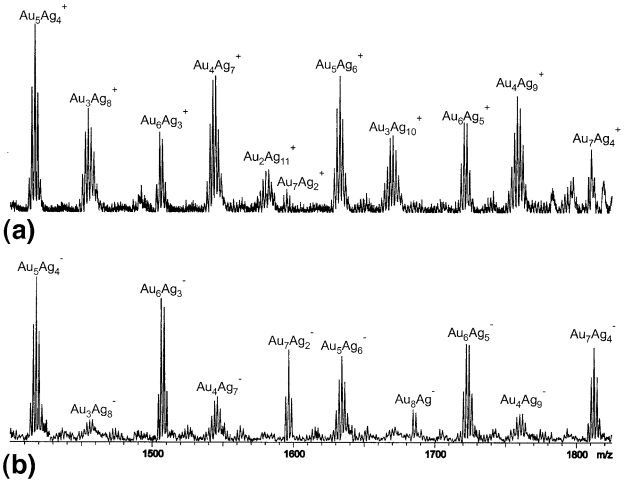

Figure 2. Partial MALDI-TOF MS spectrum of a mixture of HABA, AgTFA and $HAuCl_4$ recorded in the positive (**a**) and in the negative (**b**) reflectron mode. Experimental conditions: 15:2:1 (vol/vol) mixture of HABA (20 mg/mL), AgTFA (39 mg/mL) and $HAuCl_4$ (20 mg/mL) solutions.

Generation of Bimetallic Silver-Gold Cluster Ions Under MALDI Conditions

For the investigation of the formation of binary silver-gold clusters under MALDI conditions AgTFA and $HAuCl_4$ were mixed in different molar ratios. A large number of peaks up to the mass of 3000 Da appeared both in the positive and in the negative spectra. These peaks are due to the mixed silver-gold clusters that are present in varying compositions (corresponding to the cluster compositions of $Au_nAg_m^+$ and $A_nAg_m^-$, with $n + m \leq 20–30$) and intensities. The zoomed MALDI-TOF MS spectra with the assignments of cluster ions are plotted in Figure 2. (The full MALDI-TOF MS spectra are shown in the supplementary material). As it turns out from Figure 2, binary silver-gold cluster ions ($Au_nAg_m^+$ and $A_nAg_m^-$) with different compositions, sizes and intensities were formed, these mass spectra show rather complicated distributions of cluster compositions and sizes. To support the presence of bimetallic Au-Ag clusters ions the measured and the calculated isotopic distributions were compared. The observed and the calculated isotopic patterns for the $Au_4Ag_9^+$ cluster ion are shown in Figure 3. Since the mass accuracy up to 3000 Da is within 0.3 Da, both the mass and the isotopic pattern reflect those of pure $Au_nAg_m^+$ and $A_nAg_m^-$ cluster ions. Therefore, the formation of hydride type, e.g., $Au_nAg_mH^+$, cluster ions can be excluded or at least they formation is not significant compared to those of the pure $Au_nAg_m^+$ and $A_nAg_m^-$ cluster ions. Figure 3 shows that the observed isotopic distribution is in good agreement with the calculated one.

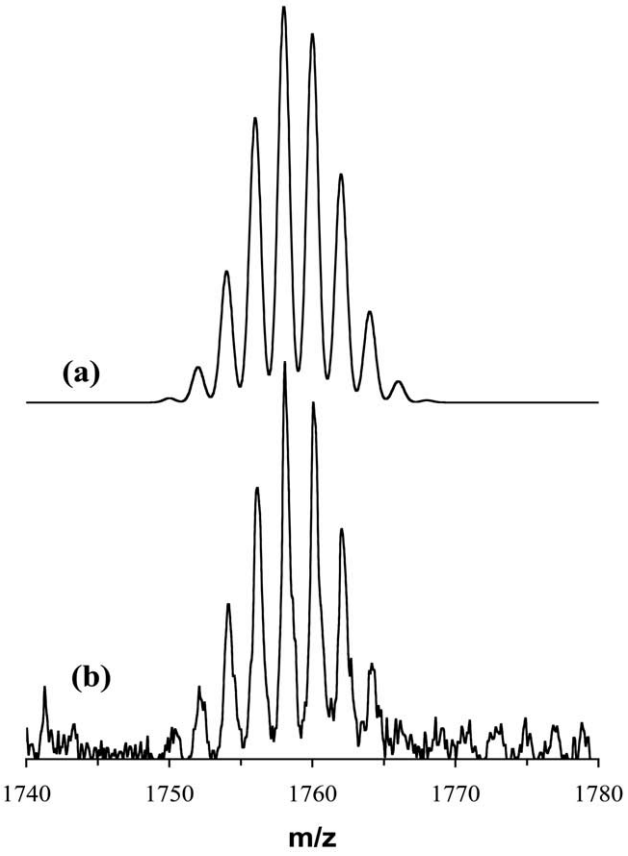

Figure 3. Calculated (**a**) and observed (**b**) isotopic distributions for the $Au_4Ag_9^+$ cluster ion produced when using a mixture of HABA, AgTFA, and $HAuCl_4$. The isotopic distributions were calculated by taking into account the Gaussian peak broadening with the experimental resolution (R) [R = 2400 fwhm (full width at half maximum)]. (Experimental conditions: see Figure 2 caption).

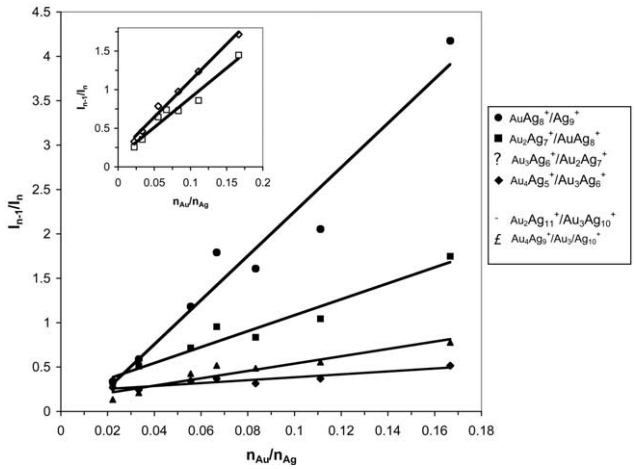

Figure 4. The intensity ratios of Au_nAg_{k-n} to $Au_{n-1}Ag_{k-n+1}$ versus n_{Au}/n_{Ag} for the positively charged cluster ions. Experimental conditions: 5:1 (vol/vol) mixture of HABA (20 mg/mL) and AgTFA (39 mg/mL) + $HAuCl_4$ (20 mg/mL) solutions.

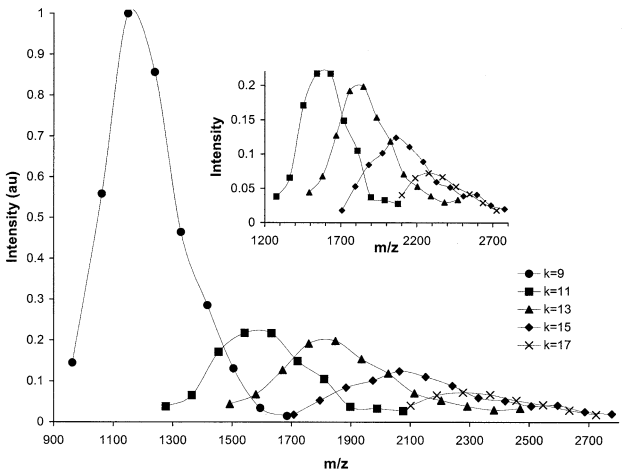

Figure 5. The intensities of the positively charged cluster ions obtained from the mass spectra. (Experimental conditions: see Figure 2 caption).

The Effect of the Initial Molar Ratio of AgTFA and $HAuCl_4$ on the Bimetallic Cluster Formation

It was observed that the resulting cluster ion intensities depended significantly on the initial molar ratio of gold to silver salts (n_{Au}/n_{Ag}). To investigate how the formation of binary Au-Ag clusters with different compositions can be controlled by the n_{Au}/n_{Ag} ratio the dependence of the intensity ratios of the $Au_nAg_m^+$ to $Au_{n+1}Ag_{m-1}^+$ cluster ions (where the value of n + m = k is constant) as a function of n_{Au}/n_{Ag} were plotted. Figure 4 shows the intensity ratios of Au_nAg_{k-n} to $Au_{n-1}Ag_{k-n+1}$ versus n_{Au}/n_{Ag} for the positively charged cluster ions. Figure 4 shows that there is a linear relationship between the corresponding intensity ratios and initial molar ratios of gold to silver salts, and a similar linear correlation was found for the negatively charged cluster ions (shown in the supplementary material). These results indicate that the formation of Au-Ag binary clusters can easily be controlled by the ratio n_{Au}/n_{Ag}. It is also evident from Figure 4 that the slopes of the lines for the intensity ratios of the $Au_nAg_{k-n}^+$ to $Au_{n-1}Ag_{k-n+1}^+$ versus n_{Au}/n_{Ag} plots decrease as the number of Au atoms (n) increase in the cluster. This finding indicates that the probability of substitution of Au by Ag atoms for a given cluster size decreases as n increases.

The Intensity Distributions of the Clusters

The intensities of the cluster ions obtained from their mass spectra can be grouped into size-distributions as indicated in Figure 5. Each group of these distributions originate from odd-number cluster ions. Within a given group, the number of Au atoms increases with increasing cluster mass, while the total number of Ag and Au atoms remains constant (k), i.e., substitution of Ag by Au atoms takes place repeatedly, going from left to the right in the mass spectrum. Similar groups can be established for the distribution of negatively charged Au-Ag cluster ions. Based on the ion intensities of the $Au_nAg_{k-n}^+$ and $Au_nAg_{k-n}^-$ cluster ions the following observations can be made: (1) We could not find any signal for an even-number cluster ion, which indicates a large difference in the stability of the odd and even number mixed cluster ions. (2) It is also seen in Figure 5 that there is a steep decrease in the ion intensity after cluster size k = 9, which is in line with the magic number predicted by the jellium model. In the case of $Au_nAg_{k-n}^-$ the intensity drop is not so significant. (The magic numbers for the single negatively charged cluster ions in this region are 7 and 19.) Observations (1) and (2) are similar to those obtained for the pure silver and gold cluster ions.

As it was shown by Villarica et al. [27] that the asymptotic solution of the Smoluchowski equation yields a lognormal distribution giving physical meaning to many observed cluster-size distributions [28, 29], therefore we used eq 1 for each intensity group of the bimetallic clusters.

$$I(n,k) = \frac{1}{n\sigma_k\sqrt{2\pi}} \exp\left[\frac{-(\ln n - \mu_k)^2}{2\sigma_k^2}\right] \quad (1)$$

where I(n,k) denotes herein the normalized intensity of the cluster ion composed of k atoms (Au and Ag atoms) and consisting of n Au atoms. μ_k and σ_k stand for the mean and the variance of the intensity distribution of cluster ions built up from k atoms, respectively.

The fitted lognormal curves, together with the normalized ion intensities of the positively charged cluster ions are plotted in Figure 6, indicating that the lognormal curves fit well to the experimental values. It is also evident from Figure 6 that the larger cluster ions accommodate more Au atoms, but their compositions remain approximately constant (except for the

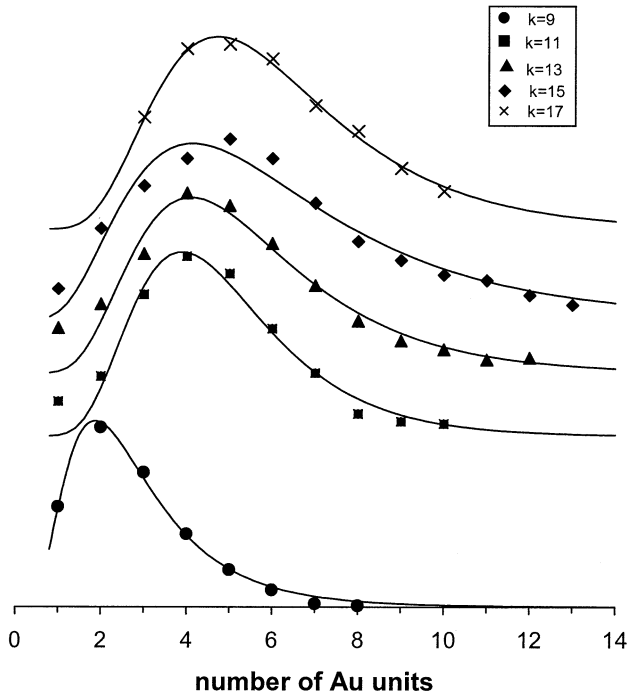

Figure 6. The normalized ion intensities of the positively charged cluster ions as a function of the number of Au atoms and the cluster size (k). The solid lines represent the fitted lognormal curves. (Experimental conditions: see Figure 2 caption).

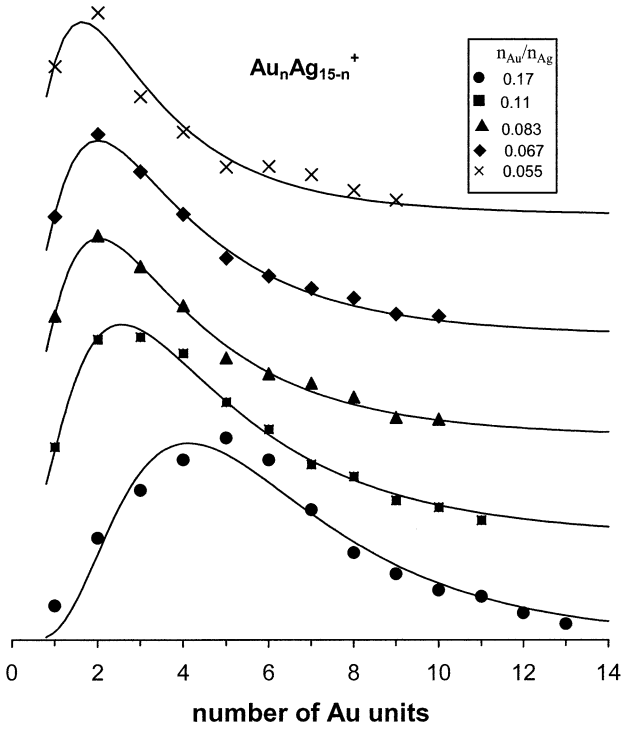

Figure 7. The normalized ion intensities of the $Au_nAg_{15-n}^+$ cluster ions as a function of the number of Au atoms and the n_{Au}/n_{Ag} ratio. The solid lines represent the fitted lognormal curves. (Experimental conditions: see Figure 5 caption).

$Au_nAg_{9-n}^+$ clusters ions). It was observed that the most probable negatively charged cluster ions incorporate more Au atoms than the positively charged ones of the same cluster size (shown in the supplementary material). On the other hand, in the case of the positively charged cluster ions, there is a considerable shift in the composition of the most probable cluster ion to higher Au content as the cluster size increases from k = 9 to k = 11. This significant shift may be attributed to the considerable difference in the stability of the cluster ions $Au_nAg_{9-n}^+$ and $Au_nAg_{11-n}^+$ (note that the magic number is 9).

Figure 7 shows the normalized cluster ion intensities for cluster size k = 15 as a function of n_{Au}/n_{Ag}. As it turns out from Figure 7, by increasing the n_{Au}/n_{Ag} ratio the composition of the most probable cluster ion shifts to higher Au content. The average composition of the clusters was calculated by eq 2,

$$x_k = \Sigma nIn/(k\Sigma In) \quad (2)$$

where x_k is the average molar fraction of gold with size of k, and I_n is the intensity of the cluster ion containing n Au atoms.

It is interesting to note that the average composition of the clusters exhibits a linear dependence on the n_{Au}/n_{Ag} ratio. By plotting x_k as a function of n_{Au}/n_{Ag} a straight line was obtained $Au_nAg_{15-n}^+$ with a slope of 1.25 and incept of 0.15 ($r^2 = 0.98$).

Fragmentation of Clusters

The fragmentations of the positively charged bimetallic Au-Ag cluster ions were also studied using the PSD MALDI-TOF MS/MS method [30, 31]. For these investigations some intensive cluster ion peaks were selected as the precursor ion for PSD. In Figure 8 the PSD MALDI-TOF MS/MS spectra of the cluster ions $Au_2Ag_3^+$ and $Au_3Ag_2^+$ are shown. As seen in Figure 8, $Au_2Ag_3^+$ yields the fragment ions by ejection of Ag,

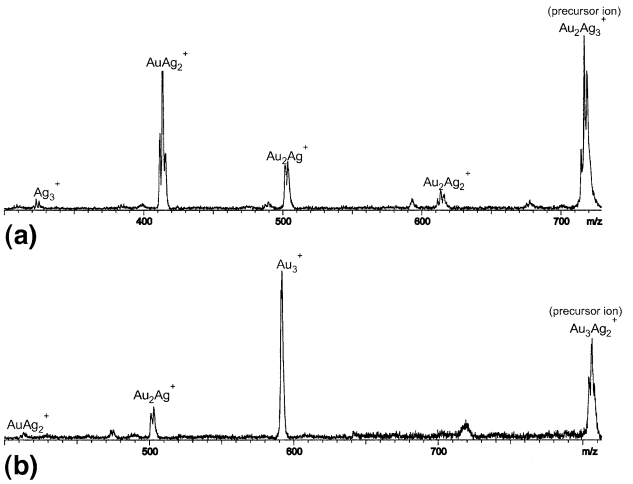

Figure 8. PSD MALDI-TOF MS/MS spectra of the $Au_2Ag_3^+$ (**a**) and $Au_3Ag_2^+$ (**b**) cluster ions.

AuAg, Ag_2, and Au_2 units. On the other hand, $Au_3Ag_2^+$ gives fragment ions by elimination of AuAg, Ag_2, and Au_2 units. No emission of a single Au atom from these two precursor ions were observed. It seems from our PSD investigations that the preferred pathway of fragmentation of the binary Au-Ag cluster ions is the loss of highly stable silver and gold dimers (the experimentally determined value of dissociation energies for Au_2 and Ag_2 are 2.29 eV [32] and 1.65 eV [33], respectively).

Conclusions

The MALDI method is very efficient for the generation of a large number of both positively and negatively charged Au-Ag cluster ions. MALDI is also an effective ion-source of these cluster ions for the study of, for example, cluster ion-molecule reactions.

It was shown that a large number of mixed cluster ions in varying compositions and sizes up to 3000 Da can be produced with the MALDI technique. The composition of the formed cluster ions can be varied with the initial molar ratio of $HAuCl_4$ to AgTFA in the solid phase. This makes possible to tailor the compositions of the mixed cluster ions for a specific demand. It was also demonstrated that the obtained cluster ion distributions can be grouped by odd-number cluster size, and each of these groups obeys the lognormal distribution.

From these observations we came to the conclusion that the mixed Au-Ag cluster ions were formed by a substitution mechanism. Substitution of Ag by Au atoms in a given sized cluster does not alter significantly the stability of the cluster ion. The proof for the above assumption is that the obtained cluster ion intensities for a given size can be fitted by the lognormal distribution which indicates that cluster ions with similar structure and stabilities were formed.

The PSD MALDI-TOF MS/MS spectra of $Au_2Ag_3^+$ and $Au_3Ag_2^+$ showed that the preferred pathway of fragmentation of Au-Ag cluster ions is the loss of stable Ag_2 and Au_2 units.

Acknowledgments

This work was financially supported by the grants T 037448, T 042740, M 28369, and M 36872, MU-00204/2001 given by OTKA (National Found for Scientific Research Development, Hungary), grant NKF3A/0036/2002 and the Bolyai János and the Békésy György Fellowship. The authors express their thanks to CELLADAM Ltd., Hungary for providing the BIFLEX III MALDI-TOF MS instrument.

References

1. Logunov, S. L.; Ahmadi, T. S.; El-Sayed, M. A.; Khoury, J. T.; Whetten, R. L. Electron Dynamics of Passivated Gold Nanocrystals Probed by Subpicosecond Transient Absorption Spectroscopy. *J. Phys. Chem. B* **1997,** *101*, 3713–3719.
2. Gaudry, M.; Lerme, J.; Cottancin, E.; Pellarin, M.; Vialle, J.-L.; Broyer, M.; Prevel, B.; Treilleux, M.; Melinon, P. Optical Properties of (AuxAg1-x)n Clusters Embedded in AluminaEvolution with Size and Stoichiometry. *Phys. Rev. B.***2001,** *64*, 085407/1–085407/7.
3. Sanchez, A.; Abbet, S.; Heiz, U.; Schneider, W. D.; Haekkinen, H.; Barnett, R. N.; Landman, Uzi. When Gold is Not Noble: Nanoscale Gold Catalysts. *J. Phys. Chem. A* **1999,** *103*, 9573–9578.
4. Schnabel, P.; Irion, M. P.; Weil, K. G. Evidence for Low-Pressure Catalysis in the Gas Phase by a Naked Metal Cluster: The Growth of Benzene Precursors on Iron (Fe^{4+}). *J. Phys. Chem.* **1991,** *95*, 9688–9694.
5. Fayet, P.; Granzer, F.; Hegenbart, G.; Moisar, E.; Pischel, B.; Woeste, L. Latent-Image Generation by Deposition of Monodisperse Silver Clusters. *Phys. Rev. Lett.* **1985,** *55*, 3002–3004.
6. Knight, W. D.; Clemenger, K.; De Heer, W. A.; Saunders, W. A.; Chou, M. Y.; Cohen, M. L. Electronic Shell Structure and Abundances of Sodium Clusters. *Phys. Rev. Lett.* **1984,** *52*, 2141–2143.
7. Hagena, O. F. Formation of Silver Clusters in Nozzle Expansions. *Zeitschrift fuer Physik D.* **1991,** *20*, 425–428.
8. Rabin, I.; Jackschath, C.; Schulze, W. Shell Effects in Singly and Multiply Charged Silver and Gold Clusters. *Zeitschrift fuer Physik D.* **1991,** *19*, 153–155.
9. Dietz, T. G.; Duncan, M. A.; Powers, D. E.; Smalley, R. E. Laser Production of Supersonic Metal Cluster Beams. *J. Chem. Phys.* **1981,** *74*, 6511–6512.
10. Bondybey, V. E.; English, J. H. Laser Excitation Spectra and Lifetimes of Diatomic Lead and Diatomic Tin Produced by YAG Laser Vaporization. *J. Chem. Phys.* **1982,** *76*, 2165–2170.
11. Weidele, H.; Vogel, M.; Herlert, A.; Kruckeberg, S.; Lievens, P.; Silverans, R. E.; Walther, C.; Schweikhard,L. Decay Pathways of Stored Metal-Cluster Anions After Collisional Activation. *Eur. Phys. J. D.* **1999,** *9*, 173–177.
12. Katakuse, I.; Ichihara, T.; Fujita, Y.; Matsuo, T.; Sakurai, T.; Matsuda, H. Mass Distributions of Negative Cluster Ions of Copper, Silver, and Gold. *Int. J. Mass Spectrom. Ion Processes* **1986**, *74*, 33–41.
13. Katakuse, I.; Ichihara, T.; Fujita, Y.; Matsuo, T.; Sakurai, T.; Matsuda, H. Mass Distributions of Copper, Silver, and Gold Clusters and Electronic Shell Structure. *Int. J. Mass Spectrom. Ion Processes* **1985**, *67*, 229–236.
14. Kruckeberg, S.; Dietrich, G.; Lutzenkirchen, K.; Schweikhard, L.; Walther, C.; Ziegler, J. Observation of Electronic and Geometric Shell Structures of Small Silver Clusters: Electron Impact Ionization/Dissociation of Size Selected Silver Clusters. *Eur. Phys. J. D.* **1999,** *9*, 169–172.
15. Staudt, C.; Heinrich, R.; Wucher, A. Formation of Large Clusters During Sputtering of Silver. *Nucl. Instr. Meth. Phys. Res. B* **2000,** *164/165*, 677–686.
16. Bauschlicher, Jr.; C. W., Langhoff, S. R.; Partridge, H. Theoretical Study of the Structures and Electron Affinities of the Dimers and Trimers of the Group IB Metals (Copper, Silver, and Gold). *J. Chem. Phys.* **1989,***91*, 2412–2419.
17. Negishi, Y.; Nakamura, Y.; Nakajima, A.; Kaya, K. Photoelectron Spectroscopy of Gold-Silver Binary Cluster Anions ($Au_nAg_m^-$; $2 \leq n + m \leq 4$). *J. Chem. Phys.* **2001,** *115*, 3657–3663.
18. Kruckeberg, S.; Dietrich, G.; Lutzenkirchen, K.; Schweikhard, L.; Walther, C.; Ziegler, J. Multiple-Collision Induced Dissociation of Trapped Silver Clusters Ag_n^+ ($2 \leq n \leq 25$). *J. Chem. Phys.* **1999,** *110*, 7216–7227.
19. Bonacic-Koutecky, V.; Burda, J.; Mitric, R.; Ge, M.; Zampella, G.; Fantucci, P. Density Functional Study of Structural and Electronic Properties of Bimetallic Silver-Gold Clusters: Comparison with Pure Gold and Silver Clusters. J. Chem. Phys. **2002,** *117*, 3120–3131.
20. Karas, M.; Hillenkamp, F. Laser Desorption Ionization of Proteins with Molecular Masses Exceeding 10,000 daltons. *Anal. Chem.* **1988,** *60*, 2299–301.

21. Tanaka, K.; Waki, H.; Ido, Y.; Akita, S.; Yoshida, Y.; Yohida, T. Protein and Polymer Analyses up to *m/z* 100,000 by Laser Ionization Time-of-Flight Mass Spectrometry. *Rapid Commun. Mass Spectrom.* **1988,** *2,* 151–153.
22. Rashidzadeh, H.; Guo, B. Generation of Large Gas-Phase Silver Cluster Ions by Laser Desorption/Ionization of Silver-Containing Salts. *Chem. Phys. Lett.* **1999,** *310,* 466–470.
23. Macha, S. F.; Limbach, P. A.; Hanton, S. D.; Owens, K. G. Silver Cluster Interferences in Matrix-Assisted Laser Desorption/Ionization (MALDI) Mass Spectrometry of Nonpolar Polymers. *J. Am. Soc. Mass Spectrom.* **2001,** *12,* 732–743.
24. Kéki, S.; Szilágyi, L. S.; Török, J.; Deák, G.; Zsuga, M. High Aggregation Number Silver Clusters by Matrix-Assisted Laser Desorption/Ionization: Role of Matrixes on the Gas-Phase Reduction of Silver Ions. J. Phys. Chem. B **2003,** *107,* 4818–4825.
25. Deák, G.; Zsuga, M.; Kelen, T. Living Polymerization of Isobutylene Initiated by p-Dicumyl Chloride/BCl_3/n-Bu4NX Systems. *Polym. Bull.* **1992,** *29,* 239–246.
26. Marquardt, D. W. Algorithm for Least Squares Estimation of Nonlinear Parameters. *J. Soc. Ind. Appl. Math.* **1963,** *11,* 431–441.
27. Villarica, M.; Casey, M. J.; Goodisman, J.; Chaiken, J. Application of Fractals and Kinetics Equations to Cluster Formation. *J. Chem. Phys.* **1993,** *98,* 4610–4625.
28. Wang, C.-R.; Huang, R.-B.; Liu, Z.-Y.; Zheng, L.-S. Lognormal Size Distributions of Elemental Clusters. *Chem. Phys. Lett.* **1994,** *227,* 103–108.
29. Wang, C.-R.; Huang, R.-B.; Liu, Z.-Y.; Zheng, L.-S. Statistical Size Distribution of Laser Generated Clusters. *Chem. Phys.* **1995,** *201,* 23–34.
30. Spengler, B.; Kirsch, D.; Kaufmann, R. Metastable Decay of Peptides and Proteins in Matrix-Assisted Laser-Desorption Mass Spectrometry. *Rapid Commun. Mass Spectrom.* **1991,** *5,* 198–202.
31. Spengler, B.; Kirsch, D.; Kaufmann, R.; Jaeger, E. Peptide Sequencing by Matrix-Assisted Laser-Desorption Mass Spectrometry. *Rapid Commun. Mass Spectrom.* **1992,** *6,* 105–108.
32. Ho, J.; Ervin, K. M.; Lineberger, W. C. Photoelectron Spectroscopy of Metal Cluster Anions: Copper, Silver, and Gold (Cu_n^-, Ag_n^-, and Au_n^-). *J. Chem. Phys.* **1990,** *93,* 6987–7002.
33. Morse, M. D. Clusters of Transition-Metal Atoms. *Chem. Rev. 86,* **1986,** 1049–1109.